Proteome profiling of cutaneous leishmaniasis lesions due to dermotropic *Leishmania donovani* in Sri Lanka

Nuwani H. Manamperi[1†], Nimesha Madhushani Edirisinghe[2†], Harshima Wijesinghe[3], Lakmali Pathiraja[4], Nishantha Pathirana[5], Vishmi Samudika Wanasinghe[2,6], Chamalka Gimhani De Silva[2,7], W. Abeyewickreme[1] and Nadira D. Karunaweera[2*]

Abstract

Background Characterization of the host response in cutaneous leishmaniasis (CL) through proteome profiling has gained limited insights into leishmaniasis research compared to that of the parasite. The primary objective of this study was to comprehensively analyze the proteomic profile of the skin lesions tissues in patients with CL, by mass spectrometry, and subsequent validation of these findings through immunohistochemical methods.

Methods Eight lesion specimens from leishmaniasis-confirmed patients and eight control skin biopsies were processed for proteomic profiling by mass spectrometry. Formalin-fixed paraffin-embedded lesion specimens from thirty patients and six control skin specimens were used for Immunohistochemistry (IHC) staining. Statistical analyses were carried out using SPSS software. The chi-square test was used to assess the association between the degree of staining for each marker and the clinical and pathological features.

Results Sixty-seven proteins exhibited significant differential expression between tissues of CL lesions and healthy controls ($p < 0.01$), representing numerous enriched biological processes within the lesion tissue, as evident by both the Kyoto Encyclopedia of Genes and Genomes (KEGG) and Reactome databases. Among these, the integrated endoplasmic reticulum stress response (IERSR) emerges as a pathway characterized by the up-regulated proteins in CL tissues compared to healthy skin. Expression of endoplasmic reticulum (ER) stress sensors, inositol-requiring enzyme-1 (IRE1), protein kinase RNA-like ER kinase (PERK) and activating transcription factor 6 (ATF6) in lesion tissue was validated by immunohistochemistry.

Conclusions In conclusion, proteomic profiling of skin lesions carried out as a discovery phase study revealed a multitude of probable immunological and pathological mechanisms operating in patients with CL in Sri Lanka, which needs to be further elaborated using more in-depth and targeted investigations. Further research exploring the intricate interplay between ER stress and CL pathophysiology may offer promising avenues for the development of novel diagnostic tools and therapeutic strategies in combating this disease.

†Nuwani H. Manamperi and Nimesha Madhushani Edirisinghe have contributed equally to this work.

*Correspondence:
Nadira D. Karunaweera
nadira@parasit.cmb.ac.lk
Full list of author information is available at the end of the article

Manamperi *et al. Clinical Proteomics*   (2024) 21:48

Page 2 of 14

Background

Human leishmaniasis, encompassing its principal clinical manifestations including cutaneous (CL), mucocutaneous (MCL), and visceral leishmaniasis (VL), poses a significant burden, particularly in tropical regions [1, 2]. The intracellular protozoan parasite *Leishmania* serves as the etiological agent of leishmaniasis and the genus *Leishmania* contains approximately 21 species that can result in a range of clinical presentations in humans depending on the infecting species [3]. Over the last three decades, Sri Lanka has witnessed the emergence of CL as a parasitic disease caused by *Leishmania donovani* zymodeme MON-37 [4].

The term "Proteome" is defined as the entire set of proteins and their alternative forms in a specific species and "proteomics" is defined as a large-scale and comprehensive study of a certain proteome [5]. In the field of leishmaniasis, proteomic profiling has predominantly focused on analyzing the proteome of the parasite, while comprehensive protein profiling of the host is less commonly performed [6]. Proteomic profiling, coupled with genome annotation techniques, has led to the identification of novel genes associated with the virulence of *Leishmania major.* These findings underscore the importance of studying both the parasite and host proteomes to gain comprehensive insights into the pathogenesis and virulence mechanisms of leishmaniasis [7].

As gene expression regulation primarily occurs at the post-transcriptional level, it necessitates the use of proteomics to effectively identify stage-specific proteins. The identification of such proteins is instrumental in elucidating the dynamic changes occurring at each different stage of the parasite's life cycle. Additionally, it is proposed that metabolomics, the study of small molecules involved in cellular metabolism, holds great promise in enhancing our comprehension of parasite biology, identifying key drug targets, and unraveling mechanisms of drug resistance. The integration of proteomic and metabolomic approaches will improve knowledge of the *Leishmania* parasite and will help the development of more effective therapeutic strategies [8]. According to Kumar et al. proteomic profiling of *L. donovani* soluble proteins have identified several novel and hypothetical proteins which can be explored as new drug targets or vaccine candidates in VL [9].

Furthermore, a study done by Hajjaran et al. on *Leishmania tropica* has identified that most responsive proteins in the visceral isolate exhibited lower abundance in the cutaneous isolate. In this study the largest clusters comprised proteins associated with carbohydrate metabolism and protein synthesis. Notably, a significant proportion of the identified proteins implicated in energy metabolism, cell signaling, and virulence demonstrated down-regulation, whereas certain proteins involved in protein folding, antioxidant defense, and proteolysis exhibited up-regulation in the visceral form [3].

Proteomic profiling of cutaneous lesions due to *Leishmania* in humans remains limited in the available literature. However, a noteworthy study on proteome profiling in CL associated with *Leishmania braziliensis* revealed the up-regulation of caspase- 9, along with the presence of caspase-3 and granzyme B in the lesions, which are known to contribute to the progression of tissue damage. Moreover, several biological functions, including apoptosis, immune response, and biosynthetic processes, were observed in both the lesions and healthy skin, but they were notably up-regulated in the lesions. The analysis of protein–protein interactions highlighted the cytotoxic T lymphocyte-mediated apoptosis of target cells as the main canonical pathway represented [6]. These findings shed light on the molecular mechanisms underlying CL lesions and provide valuable insights into the processes associated with tissue damage and immune responses in the context of *Leishmania* infections. Serum proteomic analysis in VL due to *L. donovani* has revealed differentially expressed serum proteins, which may be used as biomarkers of disease prognosis [10].

Methods

The current study aims to comprehensively analyze the proteomic profile of human CL lesions due to *L. donovani* infections in Sri Lanka and validate the biological pathways represented.

Sample collection and confirmation of diagnosis

This study received ethical approval from the Ethics Review Committee of the Faculty of Medicine, University of Kelaniya, Sri Lanka (P/99/06/2013) and was conducted adhering to the approved protocol and in agreement with the Helsinki Declaration. Patients and controls were recruited voluntarily and informed written consent was obtained before sample collection.

Patients with skin lesions suspected of CL were recruited from Base Hospital Padaviya and the Sri Lanka Army. Lesion biopsies with a diameter of 3–4 mm were obtained from the active edge of the CL lesion before

starting treatment. The diagnosis was established with light microscopy of Giemsa-stained tissue impression smears and species diagnosis was confirmed using previously established molecular methods [29]. Control skin specimens were obtained from incision sites of patients with no signs or symptoms of leishmaniasis, who underwent minor surgical procedures due to unrelated surgical causes. Skin biopsy specimens were immediately submerged in RNAlater and stored at − 20 ℃ until further analysis. Eight patient and eight control skin specimens were processed for proteomic profiling by mass spectrometry.

Samples for immunohistochemical (IHC) validation of the unfolded protein response (UPR) pathway were selected from previously archived formalin fixed paraffin embedded lesion and control specimens. Thirty lesion specimens from leishmaniasis-confirmed patients and six control specimens from patients undergoing minor surgical procedures for unrelated surgical causes were used for IHC staining. This part of the study received ethical approval from the Ethics Review Committee of the Faculty of Medicine, University of Kelaniya, Sri Lanka (Ref. No. P/21/03/2021).

Specimen transport

Specimens were transported to the Department of Pathology, Wexner Medical Center, Ohio State

University, USA, submerged in RNAlater. Dry ice was used to maintain the temperature below − 20 ℃. The amount of dry ice required for the shipment was calculated according to the time taken for air transportation, using guidelines available at http://dryiceinfo.com/shipping.htm. Triple packaged samples were shipped as Category B biological substances.

Sample processing for proteomics

Sample preparation was carried out at the Campus Chemical Instrument Center (CCIC) Mass Spectrometry and Proteomics Facility, Ohio State University, Columbus, Ohio, USA. Sample preparation was done in a Class II type A2 biosafety cabinet (NuAir, Minnesota, USA). Tissue samples stored in RNAlater were removed from the reagent, blotted on a filter paper to remove traces of RNAlater, and placed in new 1.5 ml microcentrifuge tubes (Fisher Scientific, New Hampshire, USA). Protein digestion was done using RapiGest SF Protein Digestion Surfactant (Waters, Milford, MA, USA), and samples were regarded as proteolytic resistant or hydrophobic proteins as for the manufacturer instructions and processed accordingly. To each of the tubes, 100 μL of 0.2% RapiGest SF Protein Digestion Surfactant (Waters, Milford, MA, USA) in 50 mM NH_4HCO_3 was added. Samples were sonicated in a Sonic Dismembrator (Fisher

Scientific, New Hampshire, USA) at speed 6 for 4 times and speed 5 twice, each sonication lasting 3 s. Sonicated samples were then heated at 105 ℃ in a heat block for 30 min, following which they were cooled on ice for 5 min. Samples were then vortexed for 5 min, following which they were heated at 70 ℃ for 2 h. Dithiothreitol (DDT) (ThermoFisher Scientific, USA) was added at a final concentration of 5 mM and heated at 60 ℃ for 30 min. Following this, iodoacetamide (IAA) (Acros Organics, NJ, USA) was added at 15 mM final concentration and incubated at room temperature, in the dark for 15 min to inhibit proteases. DTT reduces disulfide bonds between cysteine residues, converting them into free sulfhydryl (-SH) groups, which is essential for fully denaturing the protein and making it more amenable to enzymatic digestion, while IAA alkylates the free sulfhydryl groups to prevent them from reforming disulfide bonds, thus stabilizing the protein's denatured state and ensuring consistent and reliable analysis. For digestion of proteins, 1 μg of sequencing grade trypsin (Promega, Wisconsin, USA) was added and samples were incubated at 37 ℃ overnight.

Rapigest was precipitated by adding trifluoroacetic acid (Fisher Scientific, New Hampshire, USA) to a final concentration of 0.5% and incubating at 37 ℃ for 30 min. Samples were then centrifuged at 13,000 *g* for 15 min. The supernatant was then transferred to a microcentrifuge tube (Eppendorf®) and dried in a speed vac (Eppendorf Vacufuge Plus, Hamburg, Germany). Samples were stored at − 80 ℃ until analysis. They were then re-suspended in 50 mM acetic acid (Ultrex II Ultrapure Reagent, J.T. Baker™) and peptide concentrations were determined from their absorbance at 280 nm using a Nanodrop 1000 spectrophotometer (Thermo Fisher Scientific, USA).

Instrument protocol- tandem mass spectrometry

Tandem mass spectrometry (MS^2) was carried out using Thermo Orbitrap fusion HPLC MS−MS system (Thermo Fisher Scientific, USA). Prior to tandem mass spectrometry, samples were subjected to two −dimensional liquid chromatography (2-D LC) separation using a Thermo Scientific 2D rapid separation liquid chromatography (RSLC) high-pressure liquid chromatography (HPLC) system. A sample volume consisting of 12 ug of peptides was first separated on a 5 mm × 300 μm Ethylene Bridged Hybrid (EBH) C_{18} column with 5 μm particle size and 130 Å pore size. Solvent A was composed of 20 mM ammonium formate (Fisher Scientific New Hampshire, USA) at pH 10, and solvent B was 100% HPLC grade acetonitrile (Sigma Aldrich, Missouri, USA). Peptides were eluted from the column in eight successive fractions using 9.5, 12.4, 14.3, 16.0, 17.8, 19.7, 22.6 and 50% solvent

Manamperi *et al. Clinical Proteomics*   (2024) 21:48

Page 4 of 14

B. Each eluted fraction was then trapped, diluted, neutralized, and desalted on a μ-Precolumn Cartridge (Thermo Fisher Scientific) for the second-dimension separations performed with a 15 cm×75 cm PepMap C18 column (ThermoFisher Scientific, Waltham, MA) with 3 μm particle size and 100 Å pore size. For the Thermo Scientific 2D RSLC HPLC system, the flow rate for the analytical column was 500 μL/min. The gradient was 0 to 5 min, 2% solvent B; 5 to 38 min, 35% solvent B; 38 to 46 min, 35–55% solvent B; 46 to 47 min, 55–90% solvent B. Mobile Phase B was kept at 90% for 1 min before quickly brought back to 2%. The system was equilibrated for 11 min for the next separation.

Tandem mass spectrometry data was acquired with a spray voltage of 1.7 kV and the capillary temperature used was 275 ℃. The scan sequence of the mass spectrometer was based on the preview mode data dependent TopSpeed™ method: the analysis was programmed for a full scan recorded between *m/z* 400–1600 and an MS^2 scan to generate product ion spectra to determine the amino acid sequence in consecutive scans starting from the most abundant peaks in the spectrum in the next 3 s. To achieve high mass accuracy mass spectrometry determination, the full scan was performed in Fourier Transformation (FT) mode and the resolution was set at 120,000. The automatic gain control (AGC) target ion number for the FT full scan was set at $2×10^5$ ions, the maximum ion injection time was set at 50 ms, and the micro scan number was set at 1. Tandem mass spectrometry was performed using ion trap mode to ensure the highest signal intensity of MS^2 spectra using both collision-induced dissociation (CID) for 2+and 3+charges and electron-transfer dissociation (ETD) for 4+to 6+charges. The AGC target ion number for the ion trap MS^2 scan was set at 1000 ions, the maximum ion injection time was set at 100 ms, and the micro scan number was set at 1. The CID fragmentation energy was set to 35%. Dynamic exclusion is enabled with an exclusion duration of 15 with a repeat count of 2 within 30 s and a low mass width and high mass width of 10 ppm.

Sequence information from the MS^2 data was processed by converting.raw files into a mgf file using MS convert (ProteoWizard) and then mgf files from each of the fractions was merged into a merged file (mgf) using Merge mgf (ProteinMetrics). Isotope distributions for the precursor ions of the MS^2 spectra were de-convoluted to obtain the charge states and mono-isotopic *m/z* values of the precursor ions during the data conversion. The resulting mgf files were searched using Mascot Daemon by Matrix Science version 2.5.1 (Boston, MA, USA) and the database was searched against the human database. The mass accuracy of the precursor ions was set to 10 ppm, the accidental pick of one ^{13}C peak was also included in the search. The fragment mass tolerance was set to 0.5 Da. Considered variable modifications were oxidation (Methionine), deamidation (Asparagine and Glutamine), acetylation (Lysine), and carbamidomethylation (Cysteine) was considered as a fixed modification. Four missed cleavages for the enzyme were permitted. A decoy database was also searched to determine the false discovery rate (FDR) and peptides were filtered according to the FDR. Only proteins identified with < 1% FDR as well as a minimum of 2 peptides were reported.

Bio-informatics analysis of proteomics data

For this analysis raw data on MS/MS spectral counts were used. If a protein had a spectral count of < 6 in ≥ 90% of samples that protein was filtered out from the data analysis [30]. After filtering, 388 protein identities were left for further analysis. The Voom normalization was applied to normalize the data across all samples to reduce the bias in signal intensities from run to run. Comparison between groups was done by the 'analysis of variance' (ANOVA) method. The p-value obtained was adjusted for multiple corrections using the Benjamini–Hochberg procedure. All the proteins with an adjusted p-value < 0.01 were considered as significantly expressed between the groups compared. Significantly expressed proteins thus identified were entered into the UniProt human database [31] and converted to their corresponding gene names. Protein–protein interactions were assessed using the database 'STRING: functional protein association networks', Version 10.5 (https://string-db.org/) [32]. Pathway analysis was done using the Reactome pathway portal, version 3.2 (http://www.reactome.org) [33].

Immunohistochemical validation of IRE1, ATF6 and PERK

Immunohistochemical staining for IRE1, ATF6, and PERK was performed at Lanka Hospital Diagnostics (Pvt) Limited (PV90884), Colombo 05, Sri Lanka on paraffin-embedded tissue samples in all selected cases and controls. Tissue sections of 4 μm were cut using a microtome and the sections were mounted on positively charged slides and dried overnight in an oven at 60 ℃. The slides were dewaxed in xylene and rehydrated with 100% ethanol and 90% ethanol for 10 min each. The slides were then washed with deionized water two times for 5 min. The slides were subjected to a 25-min microwave-boiling process for antigen retrieval, using an appropriate buffer and pH as specified in Table 1.

Endogenous peroxidase was blocked by incubation in 3% hydrogen peroxide for 10 min followed by washing in deionized water and wash buffer (1×TBST). Non-specific binding was blocked by adding the blocking solution for 1 h at room temperature in a humidified chamber.

Manamperi *et al. Clinical Proteomics*   (2024) 21:48

Page 5 of 14

Table 1 Immunohistochemical protocols and scoring for IRE1, PERK, and ATF6 markers

Marker	Supplier and clone	Antigen retrieval	Primary dilution	Positive control	Interpretation	Scoring
IRE1	Abcam ab37073	Microwave in pH 6.0 citrate buffer	1:500	Small intestine	Cytoplasmic staining	Intensity score* of cytoplasmic staining × Proportion score** of cytoplasmic staining
PERK	Abcam ab79483	Microwave in pH 9.0 EDTA buffer	1:40	Colonic carcinoma	Cytoplasmic staining and nuclear staining	(Intensity score of cytoplasmic staining × Proportion score of cytoplasmic staining) + (Intensity score of nuclear staining × Proportion score of nuclear staining)
ATF6	Abcam ab203119	Microwave in pH 6.0 citrate buffer	1:250	Kidney	Nucleus and cytoplasmic staining	(Intensity score of cytoplasmic staining × Proportion score of cytoplasmic staining) + (Intensity score of nuclear staining × Proportion score of nuclear staining)

* Intensity score = 0—no staining; 1-weak staining; 2- moderate staining; 3-strong staining

** Proportion score = 0—0–5% cells; 1—6–30% cells; 2,—31–70% cells, 3—71–100% cells

The tissue sections were then incubated overnight at 4 ℃ with primary antibodies.

The antigen–antibody complex was detected by the Labeled Streptavidin–Biotin (LSAB) staining method using a biotinylated goat anti-rabbit antibody (DakoCytomation), subsequently conjugated with streptavidin horseradish peroxidase (HRP) and visualized by reacting with 3,3′-diaminobenzidine for color detection. The tissue sections were counterstained with hematoxylin. Dehydration was done by submerging the slides in 95% ethanol, 100% ethanol, and xylene twice for 10 min each respectively. Finally, the sections were mounted using a mounting medium and observed under the microscope.

The IHC-stained tissue samples were evaluated by light microscopic examination for the expression of IRE-1, PERK and ATF-6. The intensity of staining for each of the markers and the proportion of cells that expressed attaining were evaluated in 5 random fields (400 × magnification) for each section. IRE-1 was assessed for cytoplasmic staining. PERK and ATF-6 were evaluated for both cytoplasmic and nuclear staining. The proportion score was calculated as: 0, 0–5% cells were stained; 1, 6–30% cells were stained; 2, 31–70% cells were stained, and 3, 71–100% cells were stained. The staining intensity was scored as follows: 0, no staining; 1 weak staining; 2, moderate staining; 3, strong staining [34].

The overall score for IRE-1 was calculated as:

Intensity score for cytoplasmic staining
  × Proportion score cytoplasmic staining

The overall score for ATF-6 and PERK was calculated as [34, 35]:

(Intensity Score for nucleus staining
  × proportion score for nucleus staining)
  + (Intensity score for cytoplasmic staining
  × Proportion score cytoplasmic staining)

The cases that showed staining for each of the markers, IRE1, PERK, and ATF-6 were further categorized as low positivity and high positivity based on the score obtained for each of the markers. IRE -1—low positive < = 4 and high positive > 5, PERK—low positivity < = 8 and high positivity > 9, ATF-6—low positivity < = 2 and high positivity > 3. The selection of these arbitrary cut-off values is made specifically for this study, as there is no uniform threshold established in the relevant literature.

Statistical analysis

Statistical analyses were carried out using SPSS (version 25.0, SPSS Inc, Chicago, IL. USA) software. The association between the degree of staining for each marker and the clinical and pathological features was assessed using the Chi-square test. A p value < 0.05 was considered statistically significant.

Results

Proteomic profile in cutaneous leishmaniasis host tissues

A total of 1290 proteins were identified and after filtering those with a very low level of expression among the groups, 388 proteins were selected for analysis. After adjusting for multiple corrections, a total of 67 proteins (Table 2) were seen as differentially expressed between CL lesions and healthy controls (p < 0.01). Among these

Table 2 Proteins differentially expressed between cutaneous leishmaniasis lesions and normal skin

No	Gene name	Protein name	UniProt entry no	Expression change	Differential count	p value
1	OGN	Osteoglycin	P20774	Down-regulated	− 5.40804	0.00004
2	PSME1	Proteosome activator subunit 1	Q06323	Up-regulated	3.694107	0.00006
3	MYH9	Myosin heavy chain 9	P35579	Up-regulated	3.446596	0.00016
4	TMPO	Thymopoietin	P42167	Up-regulated	3.684351	0.00017
5	WARS	Tryptophanyl-tRNA synthetase	P23381	Up-regulated	4.278906	0.00018
6	HMGB2	High mobility group protein B2	P26583	Up-regulated	4.404784	0.00026
7	PDIA3	Protein disulfide isomerase family A, member 3	P30101	Up-regulated	2.543599	0.00026
8	PRKCSH	Glucosidase II subunit beta	P14314	Up-regulated	2.828193	0.00026
9	HSPE1	Heat shock 10 kDa protein 1	P61604	Up-regulated	2.54253	0.00032
10	COTL1	Coactosin-like protein1	Q14019	Up-regulated	5.028113	0.00034
11	LAP3	Leucine aminopeptidase 3	P28838	Up-regulated	3.705696	0.00034
12	RPL6	Ribosomal protein L6	Q02878	Up-regulated	2.863634	0.00034
13	MSN	Moesin	P26038	Up-regulated	3.597755	0.00034
14	IVL	Involucrin	P07476	Up regulated	3.36279	0.00053
15	TYMP	Thymidine phosphorylase	P19971	Up-regulated	4.070576	0.00053
16	CALM1	Calmodulin1	P0DP23	Up-regulated	3.270649	0.00068
17	HMGB1	High mobility group protein B1	P09429	Up-regulated	3.500734	0.00068
18	S100A9	S100 calcium-binding protein A9	P06702	Up-regulated	2.918428	0.00078
19	MZB1	Marginal zone B and B1 cell-specific protein	Q8WU39	Up-regulated	3.95914	0.00087
20	CORO1A	Coronin, actin-binding protein, 1A	P31146	Up-regulated	2.772258	0.00131
21	TNC	Tenascin C	P24821	Up- regulated	2.962339	0.00131
22	KRT17	Keratin 17	Q04695	Up-regulated	3.426447	0.00140
23	HNRNPM	Heterogeneous nuclear ribonucleoprotein M	P52272	Up-regulated	2.175227	0.00160
24	ARHGDIB	Rho GDP dissociation inhibitor (GDI) beta	P52566	Up-regulated	2.896509	0.00163
25	RPL8	Ribosomal protein L8	P62917	Up-regulated	3.17935	0.00163
26	SSB	Sjogren syndrome antigen B (Lupas La protein)	P05455	Up-regulated	3.449898	0.00163
27	KRT6A	Keratin 6A	P02538	Up-regulated	2.353024	0.00163
28	CANX	Calnexin	P27824	Up-regulated	2.013662	0.002
29	RPL4	Ribosomal protein L4	P36578	Up-regulated	2.150875	0.002
30	TPM4	Tropomyosin 4	P67936	Up-regulated	3.225065	0.0021
31	HSPA5	Heat shock 70 kDa protein 5	P11021	Up-regulated	2.543512	0.0022
32	ICAM1	Intercellular adhesion molecule 1	P05362	Up-regulated	2.675839	0.0023
33	KRT6C	Keratin 6C	P48668	Up-regulated	2.912393	0.0030
34	HCLS1	Hematopoietic lineage cell-specific protein	P14317	Up-regulated	3.138184	0.0031
35	RPL35	Ribosomal protein L35	P42766	Up-regulated	1.874303	0.0033
36	ALYREF	Aly/REF export factor	Q86V81	Up-regulated	2.72209	0.0034
37	ALDOA	Aldolase A	P04075	Up-regulated	1.903083	0.0037
38	EEF2	Eukaryotic translation elongation factor 2	P13639	Down-regulated	2.377699	0.0037
39	FLG2	Filaggrin family member 2	Q5D862	Up-regulated	− 3.81655	0.0038
40	RPL13	Ribosomal protein L13	P26373	Up-regulated	2.065239	0.0044
41	NAP1L1	Nucleosome assembly protein 1- like 1	P55209	Up-regulated	1.816704	0.0045
42	LCP1	Lymphocyte cytosolic protein 1	P13796	Up-regulated	2.809815	0.0049
43	THRAP3	Thyroid hormone receptor-associated protein 3	Q9W2Y1	Up-regulated	1.786661	0.0049
44	TPM3	Tropomyosin 3	P06753	Up-regulated	2.967553	0.0049
45	PDIA6	Protein disulfide isomerase family A, member 6	Q15084	Up-regulated	2.139193	0.005
46	GBP1	Guanylate binding protein 1	P32455	Up-regulated	3.506012	0.005
47	LSP1	Lymphocyte-specific protein 1	P33241	Up-regulated	2.886226	0.005
48	ERP29	Endoplasmic reticulum protein 29	P30040	Up-regulated	1.705599	0.0063
49	STAT1	Signal transducer and activator of transcription 1	P42224	Up-regulated	2.964521	0.0063

Manamperi *et al. Clinical Proteomics*   (2024) 21:48

Page 7 of 14

Table 2 (continued)

No	Gene name	Protein name	UniProt entry no	Expression change	Differential count	p value
50	TTR	Transthyretin	P02766	Down-regulated	− 3.45411	0.0063
51	CALR	Calreticulin	P27797	Up-regulated	2.376494	0.0064
52	NCL	Nucleolin	P19338	Up-regulated	1.789074	0.007
53	FBP1	Fructose-1,6-bisphosphatase 1	P09467	Up-regulated	2.729622	0.0082
54	AP3D1	Adaptor-related protein complex 3, delta 1 subunit	O14617	Up-regulated	2.361517	0.0082
55	HNRNPC	Heterogeneous nuclear ribonucleoprotein C (C1/C2)	P07910	Up-regulated	2.478044	0.0082
56	LMNB1	Lamin B1	P20700	Up-regulated	1.592511	0.0082
57	HLA-A	Major histocompatibility complex, class I, A	P04439	Upregulated	2.704871	0.0082
58	P4HB	Prolyl 4-hydroxylase, beta polypeptide	P07237	Up-regulated	1.870152	0.0084
59	RPL5	Ribosomal protein L5	P46777	Up-regulated	2.218306	0.0086
60	RRBP1	Ribosome binding protein 1	Q9P2E9	Up-regulated	2.275802	0.0086
61	HNRNPU	Heterogeneous nuclear ribonucleoprotein U	Q00839	Up-regulated	1.740549	0.009
62	SFPQ	Splicing factor proline/glutamine-rich	P23246	Up regulated	2.519103	0.009
63	RPS16	Ribosomal protein S16	P62249	Up-regulated	1.627651	0.0092
64	RPS19	Ribosomal protein S19	P39019	Up-regulated	1.760495	0.0092
65	S100A4	S100 calcium-binding protein A4	P26447	Up-regulated	2.500661	0.0092
66	FTL	Ferritin, a light polypeptide	P02792	Up-regulated	2.170666	0.00923
67	KRT16	Keratin 16	P08779	Up-regulated	3.083072	0.0094

Table Location—Results (Proteomic profile in cutaneous leishmaniasis host tissues

proteins, three proteins were down-regulated and 64 proteins were up-regulated.

Protein–protein interaction analysis

Protein–protein interaction network for the differentially expressed proteins between CL lesions and healthy skin demonstrated 67 nodes and 116 edges with a protein–protein interaction p value of 1×10^{-16} which is shown in Fig. 1.

Data analysis in this database provided a list of enriched pathways categorized based on Gene Ontology (GO) terms and Kyoto Encyclopedia of Genes and Genomes (KEGG) pathways. Protein–protein interactions in the KEGG pathways are significantly represented illustrated in Figs. 2 and 3.

### Pathway analysis for differentially expressed proteins by Reactome database

Gene names of significantly upregulated proteins were submitted to the Reactome pathway portal, version 3.2 (http://www.reactome.org) to identify pathways associated with these proteins. Pathways with 'entities p-value' < 0.01 were considered as significantly associated with cutaneous leishmaniasis lesions. Submitted entities are as described in Table 2.

Immunohistochemical validation of endoplasmic reticulum stress response

Most cases showed evidence of endoplasmic reticulum stress response on immunohistochemistry. Representative images in Fig. 4 illustrate the staining patterns observed. Out of thirty cases examined, 13 (43.33%) cases showed positivity for only one of the three markers assessed (IRE1, PERK, ATF-6) and 17 cases (56.67%) showed positivity for all three. The details of the expression of the individual markers are shown in Table 3. Chi-square analysis revealed a statistically significant association (p < 0.05) between the expression levels of IRE1, PERK, and ATF6 markers and both gender and histological grading in CL tissue samples. Histological grading was categorized as follows: (1) diffuse inflammatory infiltrate with parasitized macrophages, lymphocytes, and plasma cells, (2) parasitized macrophages with lymphocytes, plasma cells, and ill-formed histiocytic granulomata, and (3) a mixture of macrophages (with or without parasites), lymphocytes, plasma cells, and epithelioid granulomata.

Discussion

Evaluation of parasite, host, and vector-associated factors are central to identifying the disease pathogenesis of CL in Sri Lanka, where cutaneous manifestations are the predominantly frequent disease presentation of a usually

Manamperi *et al. Clinical Proteomics*   (2024) 21:48

Page 8 of 14
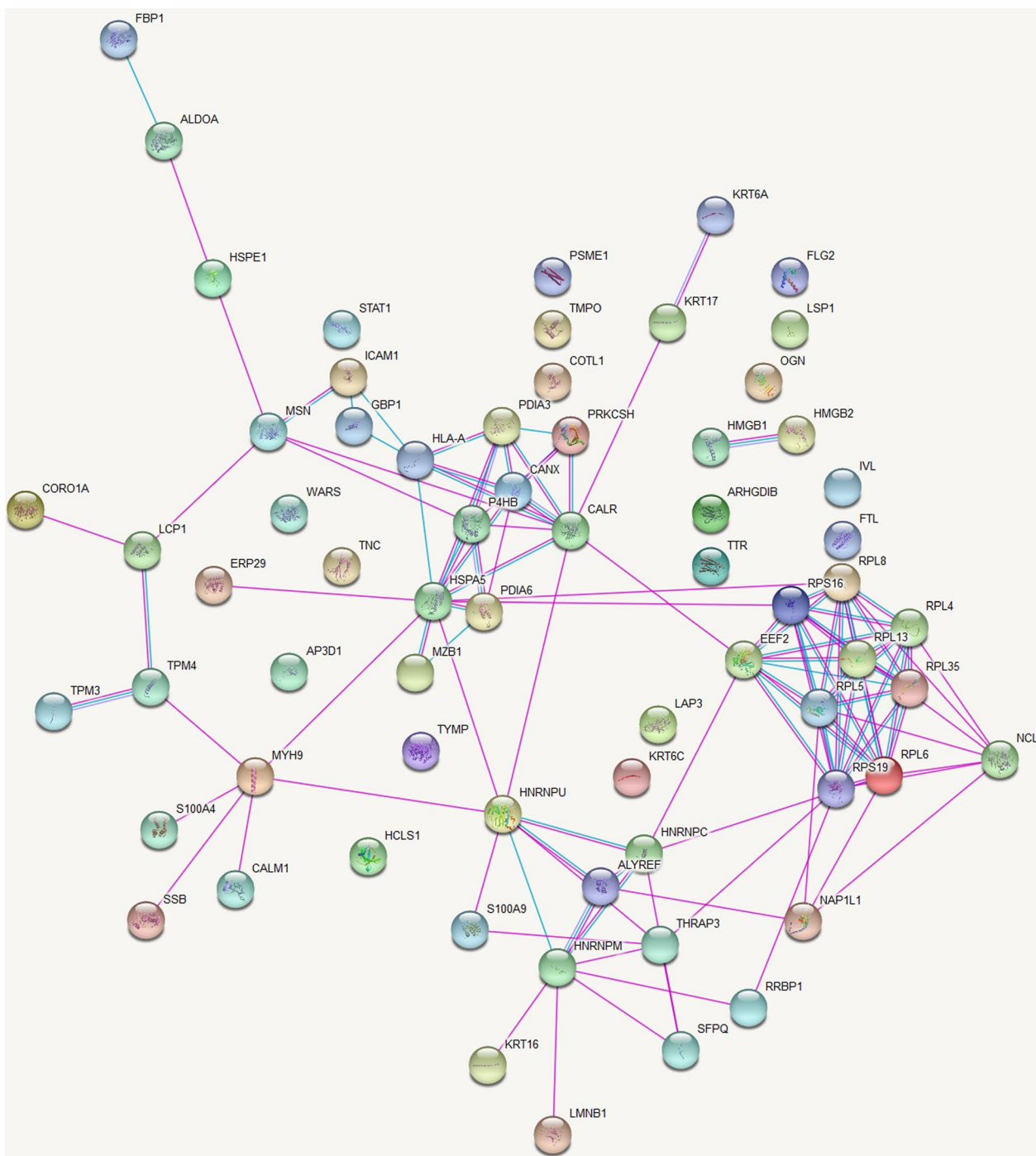
Fig. 1 Networks of protein–protein interactions between differentially expressed proteins in CL patients and healthy controls. Proteins are represented by nodes and protein–protein interactions by edges (curated in pink and experimentally determined in blue). Filled nodes indicate that some 3D structure is known or predicted, whereas empty nodes represent proteins of unknown 3D structure. Figure credit: STRING

visceralizing parasite species. Proteomics profile data obtained from this study provides insights into disease pathogenesis, as shown by enriched biological processes and pathways related to local responses.

The IERSR is one such pathway represented by the up-regulated proteins in CL patients compared to healthy skin, determined by both the KEGG and Reactome databases. Protein processing in the ER includes glycosylation
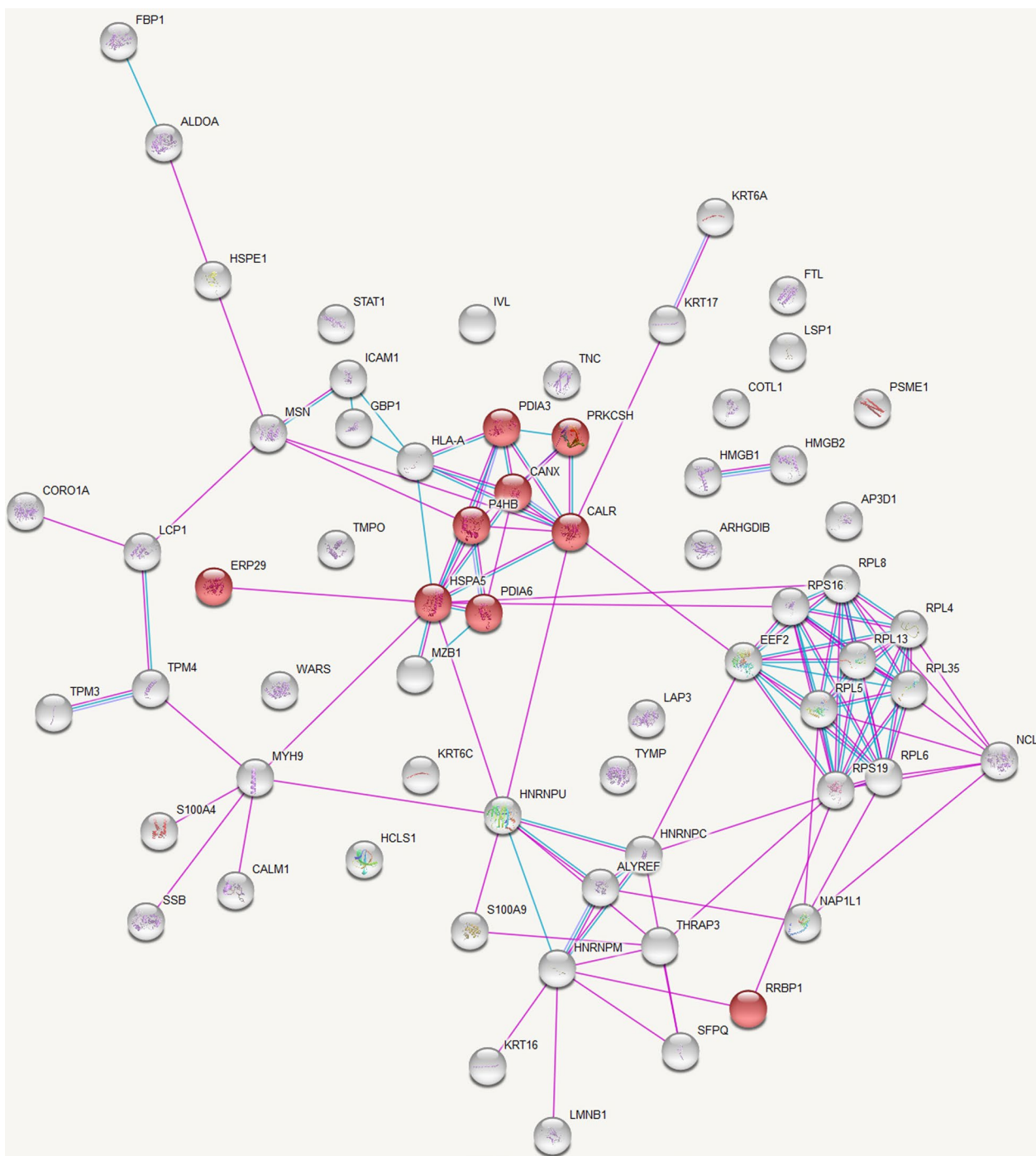
Fig. 2 KEGG Pathway Analysis of Up-Regulated Protein Interactions in Leishmaniasis: Endoplasmic Reticulum Processing Insights. Protein–protein interactions among the proteins significantly up-regulated in leishmaniasis patients compared to healthy controls with proteins involved in the KEGG pathway 'Protein processing in endoplasmic reticulum' represented in red. Figure credit: STRING

and folding of newly synthesized proteins with the help of luminal chaperons and transportation of correctly folded proteins in vesicles to the Golgi apparatus. Proteins that have not achieved proper folding are retained in the lumen of the endoplasmic reticulum, often in complex with molecular chaperones. When the protein synthesis and folding mechanism of the ER gets overwhelmed, misfolded proteins accumulate in the ER lumen, leading
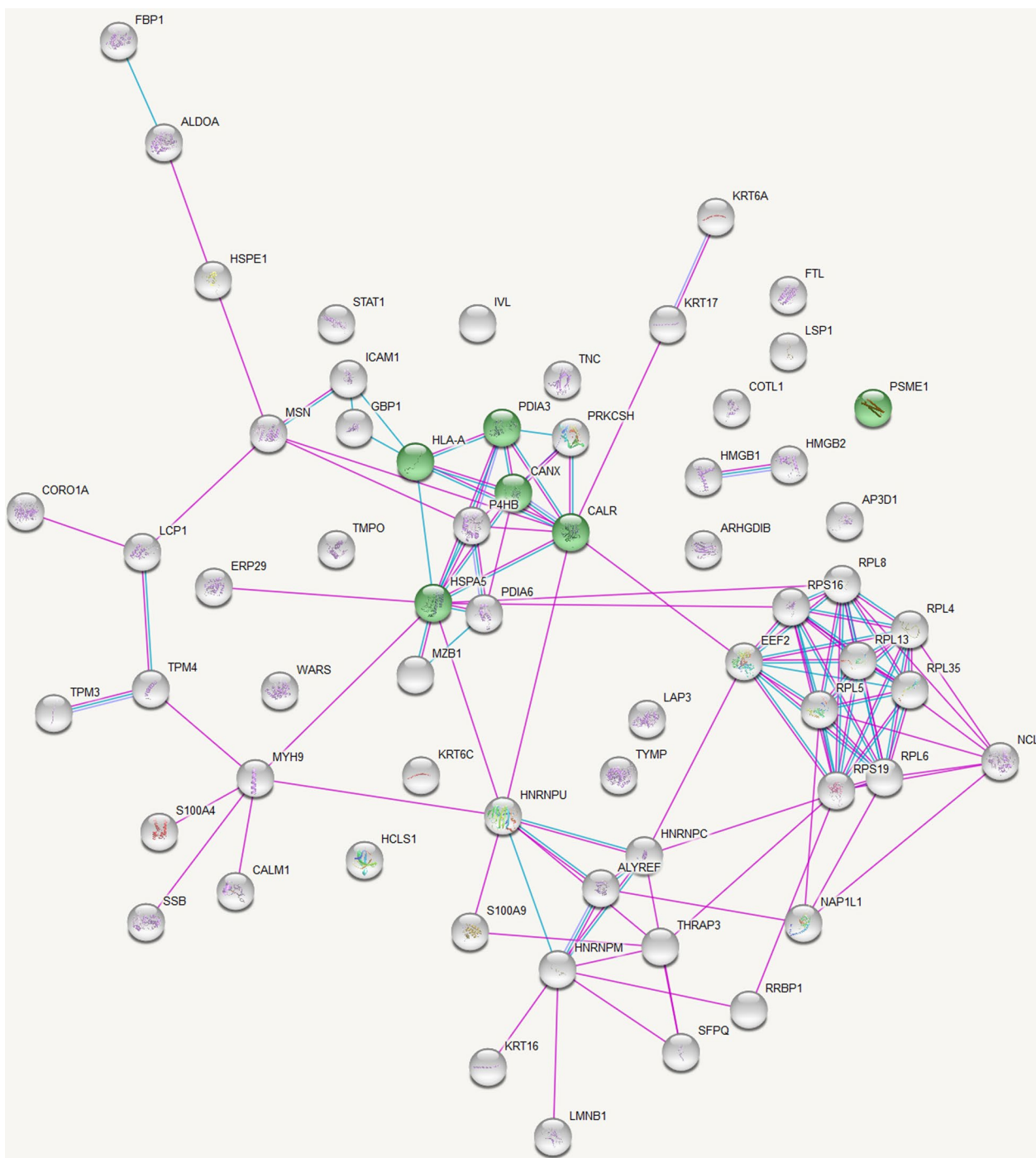
Fig. 3 KEGG Pathway Analysis of Up-Regulated Protein Interactions in Leishmaniasis: Antigen processing and presentation. Protein–protein interactions among the proteins significantly upregulated in leishmaniasis patients compared to healthy controls with proteins involved in the KEGG pathway 'Antigen processing and presentation' represented in green. Figure credit: STRING

to a state of ER stress, which in turn activates a signaling pathway known as the UPR to alleviate the ER stress. The three main stress sensors in the UPR: IRE1 pathway, PERK pathway, and ATF6 pathway, induce downstream

signaling cascades that make up the UPR. Although the UPR promotes cellular adaptations, if the ER stress is chronic these pathways signal towards cellular apoptosis. The IERSR or the UPR is proven to be associated with the
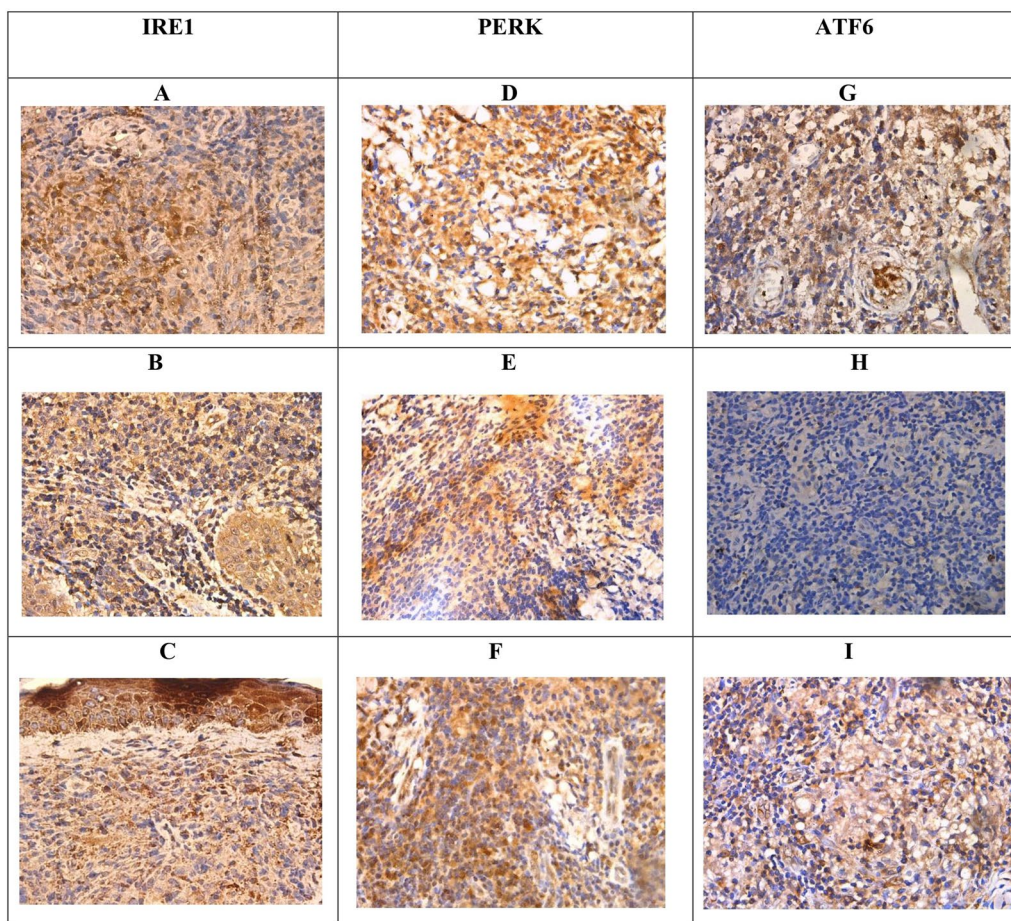
Fig. 4 Patterns of immunohistochemistry staining for IRE1, PERK, and ATF6 in samples. A—C IRE1×400. **A** Patchy nuclear and cytoplasmic positivity for IRE1. **B** Cytoplasmic positivity for IRE1, nuclear staining is absent. **C** Cytoplasmic positivity for IRE1, nuclear staining is absent. **D**–**F** PERK×400. **D** Focal nuclear and diffuse cytoplasmic positivity for PERK. **E** Cytoplasmic positivity for PERK, nuclear staining is absent. **F** Patchy nuclear and cytoplasmic positivity for PERK. **G**–**I** ATF6×400. **G** Cytoplasmic staining for ATF6, nuclear staining is absent. **H** Complete absence of nuclear and cytoplasmic staining for ATF6. **I** Patchy cytoplasmic and focal nuclear positivity for ATF6

pathology of diseases such as diabetes mellitus, neurodegeneration, inflammatory disorders, viral infection, and cancer [11]. Pathogens including bacteria and protozoa have the capacity to alter specific branches of UPR to avoid its detrimental effects.

Recent evidence suggests the involvement of specific arms of the UPR in disease pathogenesis in leishmaniasis due to several *Leishmania* species [12, 13].

Table 3 Overall score for each marker of the study sample

ER stress markers	Overall score		
	Negative	Low positivity	High positivity
IRE 1	8 (26.7%)	15 (50%)	7 (23.3%)
PERK	2 (6.7%)	15 (50%)	13 (43.3%)
ATF6	7 (23.3%)	10 (33.3%)	13 (43.3%)

Emerging evidence suggests an important role for IERSR in the pathogenesis of *L. amazonensis* and *L. braziliensis* induced CL [14, 15]. In *L. amazonensis* infection, induction of the IRE1/XBP1(X-box- binding protein-1) arm was seen as beneficial for parasite survival by creating an environment with less oxidative stress, which is mediated by the increased Interferon β (IFN-β) production. The PERK pathway is known to play a key role in autophagy and autophagy is suggested as a probable mechanism of supplying nutrition to the parasite and *L. amazonensis* is also known to induce autophagy in macrophages. It is also known that induction of a low level of stress may trigger an adaptive UPR, which increases the cellular resistance to subsequent ER stress, a process known as ER hormesis and IRE1 and PERK arms contribute to ER hormesis. Studies have shown that *L. infantum* is capable of inducing such a mild UPR in infected macrophages. Proteome profiling of CL in the present study has

Manamperi *et al. Clinical Proteomics*   (2024) 21:48

Page 12 of 14

demonstrated a significantly increased expression of proteins associated with IRE1 and ATF6 pathways suggestive of an important role played by the UPR in the pathogenesis of *L. donovani* induced CL in Sri Lanka, which is further validated by immunohistochemical staining of the ER stress sensors in lesion tissues. In this study, a significant difference was observed between the expression levels of IRE1, PERK, and ATF6 markers concerning both gender and histological grading. However, the exact role played by specific branches of the UPR in *L. donovani* infections needs to be further investigated.

The presence of an endobiont double-stranded RNA virus belonging to the *Totiviridae* family known as *Leishmaniavirus* (LRV) has been described in association with the *Leishmania (Viannia)* subgroup. The occurrence of a similar virus was described in a single isolate of *L. major* [16]. The presence of this virus has been associated with an increase in disease severity, parasite persistence, metastasis, and treatment failure [17]. Double-stranded RNA viruses are known to activate innate immune response via the Toll-like receptor 3 (TLR3) pathway which induces the secretion of IFN-β, which favors parasite survival [16]. To our knowledge, such an endobiont virus has not been demonstrated in *L. donovani*. Several pathways associated with viral infections such as viral gene expression and assembly of viral components at the budding site are represented by the upregulated proteins in CL patient samples in the present study, indicating the probability of having such an endobiont virus in the *L. donovani,* which should be further evaluated.

Furthermore, several pathways in the immune response such as class I major histocompatibility complex (MHC) mediated antigen processing and presentation, antigen processing with the cross-presentation, interferon gamma signaling, IFN-α/β signaling, IL-12 family signaling, IL-6 signaling, IL-35 signaling, and neutrophil degranulation, leucocyte migration are represented by the significantly up-regulated proteins in patient samples. Antigen presentation by class I MHC is mainly restricted to proteins synthesized within the cell and hence play a major role in viral antigen presentation to CD8+T cells. In the process of antigen cross-presentation, exogenous antigens are presented to CD8+T cells in association with class I MHC molecules instead of with MHC class II molecules [18]. This is well known for infections with intracellular pathogens with the antigen-presenting cells (APC) becoming the major source of antigen cross-presentation. APCs acquire these exogenous antigens from phagosomes (cell-associated antigens) or endosomes (soluble protein antigens). Antigenic proteins are processed and loaded onto class I MHC molecules. There are two pathways depending on the requirement for cytosolic proteases and a transporter associated with antigen processing (TAP).

The cytosolic pathway is dependent on both TAP and proteasome, whereas the vacuolar pathway is independent of both. Processed peptides are loaded onto class I MHC molecules in the ER or the phagosome [19]. In *Leishmania* infections antigens are processed in phagosomes and cross-presented via class I MHC in a TAP-independent pathway to induce a cytotoxic T-cell response. In addition to this, antigens of *Leishmania* spp. are also presented to CD4+T helper cells in association with class II MHC molecules [20]. The present study shows a more prominent antigen presentation via MHC class I and upregulation of the endosomal/vacuolar pathway important for loading antigenic peptides to MHC class I. Antigen presentation via MHC class II was not significantly represented by the upregulated proteins. This is contrary to the previously held belief that the presence of MHC class II and not class I is important for resistance to leishmaniasis [21]. The antigens presented may be originating from the *Leishmania* species itself or an endobiont virus or both. This study suggests that exogenous antigens derived from *L. donovani* may be presented via pathways dependent and independent of TAP [22].

Moreover, the significant up-regulation of Calnexin in this study suggests a potential involvement of phagosome biogenesis in the host–pathogen interactions of CL in Sri Lanka. Phagosomes are intracellular membrane-bound compartments linked to the endoplasmic reticulum, providing a protective environment where *L. donovani* can evade acquiring lysosomal properties [23].

Gene expression studies done on the cytokine response by our group [24] and other groups [25] have revealed the presence of an up-regulated T helper cells (Th1) response in CL in Sri Lanka. The current study on proteome profiling of CL lesions has further proven the presence of an up-regulated Th1 response in *L. donovani* induced CL in Sri Lanka at the post-translational stage. Four proteins associated with the IFN-γ signaling pathway were seen to be significantly upregulated in patient tissues compared to healthy controls and six proteins in the IL-12 signaling pathway were also significantly upregulated. The action of IL-12 is important in bridging the innate and adaptive arms of the host immune response [26]. The IL-12 family of cytokines consists of IL-12 and IL-23 which are pro-inflammatory, and IL-27 and IL-35 which are immune-suppressive and regulate the immune response in autoimmune and infectious diseases [27]. Pathway analysis in this study has shown the presence of IL-27 and IL-35 signaling pathways, which need to be validated and quantified further to decipher their extent of involvement in the immune response against CL.

In addition, processes involved in the protein translation in ribosomes and cytoplasmic transport are also significantly up-regulated indicating the active

inflammatory milieu created in the lesion compared to the healthy skin. Also, the current study reveals a notable up-regulation in the pathway of apoptosis-induced DNA fragmentation. Even though histological evidence of apoptosis or necrosis is not very prominent in CL due to *L. donovani* in Sri Lanka [28], this study points to the presence of apoptosis, possibly at a low magnitude in the lesions.

Conclusions

Leishmania spp. parasites comprise a diverse group of protozoans that lead to a range of disease manifestations. The immunological responses to these parasites are highly intricate. This complexity hinges on factors like the causative species and possibly the strain involved. In Sri Lanka, CL has emerged as an established vector-borne parasitic disease, characterized by a fascinating clinical presentation. This study which investigates the proteomic profiling of leishmaniasis lesions revealed a multitude of probable immunological and pathological mechanisms operating in patients with CL in Sri Lanka such as the unfolded protein response, a probable association of an endosymbiont virus in the parasite, IFN-α/β signaling, and phagosome biogenesis, which need to be further elaborated using more in-depth and targeted investigations.

Abbreviations
CL	Cutaneous leishmaniasis
IHC	Immunohistochemistry
KEGG	Kyoto Encyclopedia of Genes and Genomes
IERSR	Integrated endoplasmic reticulum stress response
ER	Endoplasmic reticulum
IRE 1	Inositol-requiring enzyme-1
PERK	Protein Kinase RNA-like ER Kinase
ATF 6	Activating transcription factor 6
MCL	Mucocutaneous Leishmaniasis
VL	Visceral leishmaniasis
UPR	Unfolded protein response
CCIC	Campus Chemical Instrument Center
MS^2	Tandem mass spectrometry
2-D LC	Two –Dimensional Liquid Chromatography
RSLC	Rapid separation liquid chromatography
HPLC	High-pressure liquid chromatography
FT	Fourier Transformation
AGC	Automatic gain control
CID	Collision-induced dissociation
ETD	Electron-transfer dissociation
FDR	False discovery rate
LSAB	Labeled Streptavidin–Biotin
HRP	Horseradish peroxidase
XBP 1	X-box- binding protein-1
IFN- β	Interferon β
LRV	*Leishmaniavirus*
TLR3	Toll-like receptor 3
MHC	Major histocompatibility complex
IL	Interleukin
APC	Antigen-presenting cells
TAP	Transporter associated with antigen processing
Th1	T helper cells

Availability of data and materials
The datasets used during the current study are available from the corresponding author upon reasonable request.

Declarations

Ethics approval and consent to participate
This study was approved by the Ethics Review Committee of the Faculty of Medicine, University of Kelaniya, Sri Lanka (for proteomics work—Ref NO. P/99/06/2013), (IHC work—Ref. No. P/21/03/2021). All participants provided written informed consent.

Consent for publication
Not applicable**.**

Competing interests
The authors have declared that no competing interests exist.

Author details
[1]Department of Parasitology, Faculty of Medicine, University of Kelaniya, Kelaniya, Sri Lanka. [2]Department of Parasitology, Faculty of Medicine, University of Colombo, Colombo 08, Sri Lanka. [3]Department of Pathology, Faculty of Medicine, University of Colombo, Colombo 08, Sri Lanka. [4]Base Hospital, Padaviya, Sri Lanka. [5]Sri Lanka Army Medical Services, Colombo, Sri Lanka. [6]Present Address: Department of Physiology and Cell Biology, Dorothy M. Davis Heart and Lung Research Institute, The Ohio State University, Columbus, USA. [7]Present Address: Department of Physiology and Neurobiology, University of Connecticut, Storrs, USA.

References
1. Shamkhi GJ, Alali S. Review article: impact of Leishmania spp. on public health. Tex J Agric Biol Sci. 2023;15:26–36.
2. Valigurová A, Kolářová I. Unrevealing the mystery of latent Leishmaniasis: what cells can host Leishmania? Pathogens. 2023;12:246.
3. Hajjaran H, Mousavi P, Burchmore R, Mohebali M, Mohammadi Bazargani M, Hosseini Salekdeh G, et al. Comparative proteomic profiling of Leishmania tropica: Investigation of a case infected with simultaneous cutaneous and viscerotropic leishmaniasis by 2-dimentional electrophoresis and mass spectrometry. Iran J Parasitol. 2015;10:366–80.

4.   Karunaweera ND, Pratlong F, Siriwardane HVYD, Ihalamulla RL, Dedet JP. Sri Lankan cutaneous leishmaniasis is caused by *Leishmania donovani* zymodeme MON-37. Trans R Soc Trop Med Hyg. 2003;97:380–1.
5.   Li S, Tang H. Computational methods in mass spectrometry-based proteomics. Adv Exp Med Biol. 2016;939:63–89.
6.   Da Silva SC, Attarha S, Saini RK, Boaventura V, Costa J, Khouri R, et al. Proteome profiling of human cutaneous leishmaniasis lesion. J Invest Dermatol. 2015;135:400–10.
7.   Pawar H, Renuse S, Khobragade SN, Chavan S, Sathe G, Kumar P, et al. Neglected tropical diseases and omics science: proteogenomics analysis of the promastigote stage of *Leishmania major* parasite. Omi A J Integr Biol. 2014;18:499–512.
8.   Scheltema RA, Decuypere S, T'Kindt R, Dujardin JC, Coombs GH, Breitling R. The potential of metabolomics for Leishmania research in the post-genomics era. Parasitology. 2010;137:1291–302.
9.   Kumar A, Misra P, Sisodia B, Shasany AK, Sundar S, Dube A. Mass spectrometry-based proteomic analysis of *Leishmania donovani* soluble proteins in Indian clinical isolate. Pathog Dis. 2014;70:84–7.
10. Rukmangadachar LA, Kataria J, Hariprasad G, Srinivasan JC, Srinivasan A. Two-dimensional difference gel electrophoresis (DIGE) analysis of sera from visceral leishmaniasis patients. Clin Proteomics. 2011. https://doi.org/10.1186/1559-0275-8-4.
11. Oakes SA, Papa FR. The role of endoplasmic reticulum stress in human pathology. Annu Rev Pathol Mech Dis. 2015;10:173–94.
12. Bravo R, Parra V, Gatica D, Rodriguez AE, Torrealba N, Paredes F, et al. Endoplasmic reticulum and the unfolded protein response. Dynamics and metabolic integration. Int Rev Cell Mol Biol. 2013;301:215–90.
13. Urra H, Dufey E, Lisbona F, Rojas-Rivera D, Hetz C. When ER stress reaches a dead end. Biochim Biophys Acta—Mol Cell Res. 2013;1833:3507–17. https://doi.org/10.1016/j.bbamcr.2013.07.024.
14. Dias-Teixeira KL, Pereira RM, Silva JS, Fasel N, Aktas BH, Lopes UG. Unveiling the role of the integrated endoplasmic reticulum stress response in Leishmania infection—future perspectives. Front Immunol. 2016;7:6–9.
15. Dias-Teixeira KL, Calegari-Silva TC, Medina JM, Vivarini ÁC, Cavalcanti Á, Teteo N, et al. Emerging role for the PERK/eIF2α/ATF4 in human cutaneous leishmaniasis. Sci Rep. 2017;7:1–11.
16. Hartley MA, Ronet C, Zangger H, Beverley SM, Fasel N. Leishmania RNA virus: when the host pays the toll. Front Cell Infect Microbiol. 2012;2:99.
17. Adaui V, Lye LF, Akopyants NS, Zimic M, Llanos-Cuentas A, Garcia L, et al. Association of the endobiont double-stranded RNA virus LRV1 with treatment failure for human leishmaniasis caused by leishmania braziliensis in Peru and Bolivia. J Infect Dis. 2016;213:112–21.
18. Groothuis TAM, Neefjes J. The many roads to cross-presentation. J Exp Med. 2005;202:1313–8.
19. Blanchard N, Shastri N. Cross-presentation of peptides from intracellular pathogens by MHC class I molecules. Ann N Y Acad Sci. 2010;1183:237–50.
20. Goldszmid RS, Sher A. Processing and presentation of antigens derived from intracellular protozoan parasites. Curr Opin Immunol. 2010;22:118–23.
21. Alexander J, Satoskar AR, Russell DG. Leishmania species: models of intracellular parasitism. J Cell Sci. 1999;112:2993–3002.
22. Mantegazza AR, Magalhaes JG, Amigorena S, Marks MS. Presentation of phagocytosed antigens by MHC class I and II. Traffic. 2013;14:135–52.
23. Kaye P, Scott P. Leishmaniasis : complexity at the host—pathogen interface. Nat Publ Gr. 2011;9:604–15. https://doi.org/10.1038/nrmicro2608.
24. Manamperi NH, Oghumu S, Pathirana N, de Silva MVC, Abeyewickreme W, Satoskar AR, et al. In situ immunopathological changes in cutaneous leishmaniasis due to Leishmania donovani. Parasite Immunol. 2017;39:1–9.
25. Atapattu D, Iddawela D, Adikari S, Wickramasinghe S, Bandara L, Samaraweera S. The first documentation of the immune response to cutaneous leishmaniasis caused by Leishmania donovani in Sri Lanka. Sri Lankan J Infect Dis. 2017;7:76.
26. Abbas AK, Lichtman AH. Cell Mol Immunol. 5th edn. Philadelphia, Elsevie. 2005;108-9.
27. Egwuagu CE, Yu CR, Sun L, Wang R. Interleukin 35: critical regulator of immunity and lymphocyte-mediated diseases. Cytokine Growth Factor Rev. 2015;26:587–93. https://doi.org/10.1016/j.cytogfr.2015.07.013.
28. Wijesinghe H, Gunathilaka N, Semege S, Pathirana N, Manamperi N, De Silva C, et al. Histopathology of cutaneous leishmaniasis caused by *Leishmania donovani* in Sri Lanka. Biomed Res Int. 2020;2020:1–8.
29. Deepachandi B, Weerasinghe S, Soysa P, Karunaweera N, Siriwardana Y. A highly sensitive modified nested PCR to enhance case detection in leishmaniasis. BMC Infect Dis. 2019;19:1–10.
30. Lundgren DH, Hwang SI, Wu L, Han DK. Role of spectral counting in quantitative proteomics. Expert Rev Proteom. 2010;7:39–53.
31. Bateman A, Martin MJ, O'Donovan C, Magrane M, Alpi E, Antunes R, et al. UniProt: the universal protein knowledgebase. Nucleic Acids Res. 2017;45:D158–69.
32. Szklarczyk D, Franceschini A, Wyder S, Forslund K, Heller D, Huerta-Cepas J, et al. STRING v10: protein-protein interaction networks, integrated over the tree of life. Nucleic Acids Res. 2015;43:D447–52.
33. Fabregat A, Jupe S, Matthews L, Sidiropoulos K, Gillespie M, Garapati P, et al. The reactome pathway knowledgebase. Nucleic Acids Res. 2018;46:D649–55.
34. Hanaoka M, Ishikawa T, Ishiguro M, Tokura M, Yamauchi S, Kikuchi A, et al. Expression of ATF6 as a marker of pre-cancerous atypical change in ulcerative colitis-associated colorectal cancer: a potential role in the management of dysplasia. J Gastroenterol. 2018;53:631–41.
35. Levidou G, Saetta AA, Gigelou F, Karlou M, Papanastasiou P, Stamatelli A, et al. ERK/pERK expression and B-raf mutations in colon adenocarcinomas: Correlation with clinicopathological characteristics. World J Surg Oncol. 2012;10:1–11.

Publisher's Note